

Geology

First active hydrothermal vents on an ultraslow-spreading center: Southwest Indian Ridge

Chunhui Tao, Jian Lin, Shiqin Guo, Yongshun John Chen, Guanghai Wu, Xiqiu Han, Christopher R. German, Dana R. Yoerger, Ning Zhou, Huaiming Li, Xin Su, Jian Zhu and and the DY115-19 (Legs 1–2) and DY115-20 (Legs 4–7) Science Parties

Geology 2012;40;47-50
doi: 10.1130/G32389.1

Email alerting services click www.gsapubs.org/cgi/alerts to receive free e-mail alerts when new articles cite this article

Subscribe click www.gsapubs.org/subscriptions/ to subscribe to *Geology*

Permission request click <http://www.geosociety.org/pubs/copyrt.htm#gsa> to contact GSA

Copyright not claimed on content prepared wholly by U.S. government employees within scope of their employment. Individual scientists are hereby granted permission, without fees or further requests to GSA, to use a single figure, a single table, and/or a brief paragraph of text in subsequent works and to make unlimited copies of items in GSA's journals for noncommercial use in classrooms to further education and science. This file may not be posted to any Web site, but authors may post the abstracts only of their articles on their own or their organization's Web site providing the posting includes a reference to the article's full citation. GSA provides this and other forums for the presentation of diverse opinions and positions by scientists worldwide, regardless of their race, citizenship, gender, religion, or political viewpoint. Opinions presented in this publication do not reflect official positions of the Society.

Notes

First active hydrothermal vents on an ultraslow-spreading center: Southwest Indian Ridge

Chunhui Tao^{1*}, Jian Lin^{2*}, Shiqin Guo³, Yongshun John Chen⁴, Guanghai Wu¹, Xiqu Han¹, Christopher R. German², Dana R. Yoerger⁵, Ning Zhou³, Huaiming Li¹, Xin Su⁶, Jian Zhu⁴, and the DY115-19 (Legs 1–2) and DY115-20 (Legs 4–7) Science Parties

¹Key Laboratory of Submarine Geosciences, Second Institute of Oceanography, SOA, Hangzhou 310012, China

²Department of Geology and Geophysics, Woods Hole Oceanographic Institution, Woods Hole, Massachusetts 02543, USA

³China Ocean Mineral Resources R&D Association, Beijing 100860, China

⁴Department of Geophysics, School of Earth & Space Sciences, Peking University, Beijing 100871, China

⁵Department of Applied Physics and Ocean Engineering, Woods Hole Oceanographic Institution, Woods Hole, Massachusetts 02543, USA

⁶China University of Geosciences, School of Ocean Sciences, Beijing 100083, China

ABSTRACT

The ultraslow-spreading Southwest Indian Ridge is a major tectonic province, representing one of the important end-member mid-ocean-ridge types for its very slow and oblique spreading, and providing the only known route for migration of chemosynthetic deep-sea vent fauna between the Atlantic and Indian Oceans. We report the investigation of the first active high-temperature hydrothermal field found on any ultraslow mid-ocean ridge worldwide. Located on Southwest Indian Ridge at 37°47'S, 49°39'E, it consists of three zones extending ~1000 m laterally, and it is one of four recently discovered active and inactive vent sites within a 250-km-long magmatically robust section. Our results provide the first direct evidence for potentially widespread distribution of hydrothermal activity along ultraslow-spreading ridges—at least along magmatically robust segments. This implies that the segment sections with excess heat from enhanced magmatism and suitable crustal permeability along slow and ultraslow ridges might be the most promising areas for searching for hydrothermal activities. It is surprising that the special vent fauna appear to indicate some complex affinity to those on the Central Indian Ridge, southern Mid-Atlantic Ridge, and the southwest Pacific Ocean.

INTRODUCTION

The cumulative length of Earth's ultraslow-spreading ridges, where the full seafloor spreading rate is less than 16 mm/yr, is more than 15,000 km, representing ~20% of the global mid-ocean-ridge system (Solomon, 1989). Thus, ultraslow ridges constitute a major component of Earth's tectonic plate boundaries and the associated heat transfer from the mantle to oceans. Because of their remote locations, most ultraslow ridges, which include the Gakkel Ridge in the Arctic Ocean and the Southwest Indian Ridge (SWIR), have remained extremely difficult to investigate (Dick et al., 2003; Edmonds et al., 2003; Baker and German, 2004). Only with a significant improvement in underwater technologies, coupled with an increasing commitment toward international collaboration in the past decade, has significant progress in the study of ultraslow ridges begun to be made (Snow and Edmond, 2007). The first indirect evidence for the presence of hydrothermal venting, from water-column anomalies overlying the eastern SWIR, was obtained in 1997 (German et al., 1998). Further evidence for additional hydrothermal plumes along the

western SWIR and recovery of inactive sulfide deposits and/or metalliferous sediments from both the eastern and western SWIR followed in subsequent years (Fujimoto et al., 1999; Münch et al., 2001; Bach et al., 2002; German, 2003).

Indications of strong hydrothermal plumes were detected along the central eastern SWIR near 50°E (Lin and Zhang, 2006), leading to the investigations in 2007 by *D/V Dayang Yihao*. Subsequently, some hydrothermal fields were found along the ultraslow-spreading ridges, like the Gakkel Ridge in the Arctic Ocean (Pedersen et al., 2010) and the Cayman Trough in the Caribbean Sea (German et al., 2010).

GEOLOGICAL SETTING

Our study area on the SWIR is centered on spreading segments 27–29 between the Indomed and Gallieni transform faults (Sauter et al., 2001) (Figs. 1 and 2). Geophysical surveys of this region (Georgen et al., 2001; Sauter et al., 2001, 2004; Tao et al., 2009) have revealed that this part of the SWIR has experienced a dramatic increase in magma supply since 8–10 Ma. The oceanic lithosphere younger than this age is associated with significantly shallower seafloor and thicker

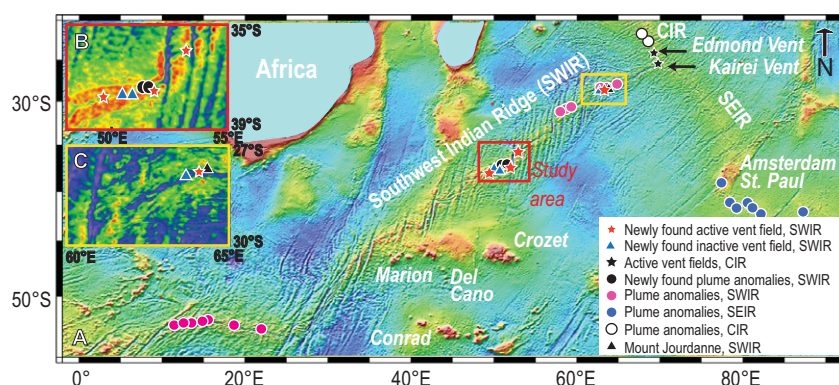


Figure 1. Location of the study area on the Southwest Indian Ridge (SWIR). **A:** Study area (red box) is in the central eastern part of the SWIR, ~900 km north of the Crozet hotspot (satellite gravimetric map). Black stars are the two known active fields: Kairei (Hashimoto et al., 2001) and Edmond (Van Dover et al., 2001) sites, on the Central Indian Ridge (CIR). Circles are the hydrothermal anomalies located along the SWIR, CIR, and Southeast Indian Ridge (SEIR) (German et al., 1998; Münch et al., 2001; German, 2003; Fujimoto et al., 1999; Bach et al., 2002; Lin and Zhang, 2006; Tao et al., 2009; Herzig and Plüger, 1988; Scheirer et al., 1998; Plüger et al., 1990). Red stars and blue triangles are newly found active and inactive vent fields, respectively. **B** and **C:** Close-up maps of the two study areas on the SWIR near 47°E–55°E (**B**) and 60°E–65°E (**C**), respectively (bathymetric map).

*E-mails: taochunhuimail@163.com; jlin@whoi.edu.

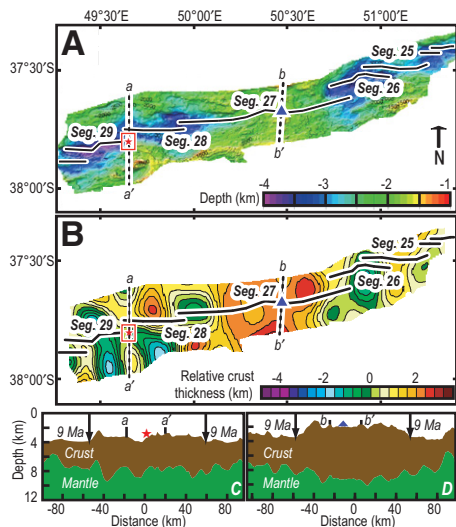


Figure 2. Location of the newly found vent fields. A: Bathymetric map showing location of the active (red star) and inactive (blue triangle) fields (Tao et al., 2008, 2009). **B:** Map of gravity-derived relative crust thickness (modified from Sauter et al., 2004) showing that the active field is located at a nontransform discontinuity, while the inactive fields at 50°28'E and 51°0.55'E are located in regions of excess and moderate crust thickness, respectively. **C and D:** Cross-axis profiles showing seafloor depth and gravity-derived relative crustal thickness through the active (C) and inactive field (D) at 49°39'E and 50°28'E, respectively. Since ca. 9 Ma, this region has been experiencing relatively robust magmatism as reflected in thickened crust (Sauter et al., 2004).

crust than that of older lithosphere (Figs. 2C and 2D). The 80-km-long segment 27 is magnetically the most robust spreading segment in this region. The seafloor is as shallow as 1700 m at the segment center, where the axial rift valley disappears (Figs. 2A and 2D) and the crust is 3 km thicker than at the segment ends (Figs. 2B and 2D). In contrast, the midpoint of the 32-km-long segment 28 is at a depth of 3000 m (Fig. 2A). The crustal thickness is also very asymmetric across segment 28 (Fig. 2B). The high topography south of segment 28 is associated with relatively thin crust, implying a dynamically uplifted origin as inside corner crust. Segment 29 is associated with even greater seafloor depth and thinner crust (Figs. 2A and 2B).

HYDROTHERMAL VENTS AT 49°E–53°E, SOUTHWEST INDIAN RIDGE

In February–March 2007, during the Chinese DY115–19 cruise, we determined the precise location of the active vent field at 49°39'E using a combination of water-column surveys, deep-tow video imaging, and three phases of investigation using the autonomous underwater vehicle *ABE* (Autonomous Benthic Explorer). Near-bottom water-column anomalies in tem-

perature, turbidity, and methane concentrations were detected first, and video images of metalliferous sediments were captured. We then determined the precise location of three active venting areas (areas 1, 2, and 3 in Fig. 3B) in the S (southern) zone and completed visual geological and biological characterization of this zone (Fig. 4C) (see the GSA Data Repository¹). In November 2008–February 2009, during the DY115–20 cruise, we identified the M (middle) active venting zone, as well as the N (northern) zone, where diffuse flow at the seafloor and overlying water-column anomalies were observed (Fig. 3B). The inactive field toward the center of segment 27 (Figs. 2A and 3C) was also discovered at 50°28'E during this later cruise, using deep-tow video imaging combined with temperature, redox potential (Eh), methane sensors, and TV grab sampling. In addition to the 49°39'E active vent site and 50°28'E inactive site, two more vent sites (at 51°0.55'E, 37°36.48'S and 51°43.92'E, 37°27.96'S) and two water-column anomalies (at 51°24.6'E, 37°25.8'S and 51°37.2'E, 37°26.4'S) were found in the section of the SWIR between 49°E and 52°E during the following Legs 5–7 of the Chinese DY115–20 expedition (Tao et al., 2009) (Figs. 1 and 2A).

The 49°39'E active field is located on the western flank of a north-south-trending topographic high abutting and paralleling the nontransform offset between segments 28 and 29 (Fig. 2A). The vent-hosting topographic high is between two areas of relatively thin crust (Fig. 2B). The depth of the active vent field is 2760 m. Contours

of relatively high crustal magnetization appear to extend all the way from the center of segment 28 to the topographic high that hosts the active venting (Sauter et al., 2004), implying that this north-south-trending ridge-like feature might be associated with recent seafloor volcanism and/or an anomalously thick layer of high magnetization. The *ABE* photographic survey of the S zone seafloor revealed abundant basaltic pillows along the north-south topography high, as well as basaltic talus along the flanks of the S zone. In contrast, the 50°28'E inactive field is located at the midpoint of segment 27 in an area of relatively thick crust, with no axial rift valley, and a very shallow depth of 1739 m (Figs. 2B and 3C).

The S zone is ~120 m across, based on direct evidence from seafloor photographic observations of chimney structures and associated fauna as well as in situ measurements of water-column temperature and turbidity anomalies (Figs. 3A, 3B, and 4). *ABE* sensors measured temperature anomalies (>2.5 °C) in three discrete venting areas (marked 1, 2, and 3 in Fig. 4C). At areas 1 and 2, photographs from *ABE* revealed black smoke rising from the seafloor (black ellipses in Fig. 4C) in the location of the temperature anomalies. No black smoke was imaged in area 3, although high-temperature measurements were extensive, and sulfide material was apparent in the photographic record (Fig. 4C). We hypothesize that the tops of the venting chimneys rose higher than the *ABE* flying height of 5 m from bottom, so that the high-temperature fluid and plumes were not imaged by *ABE*. Sulfide depos-

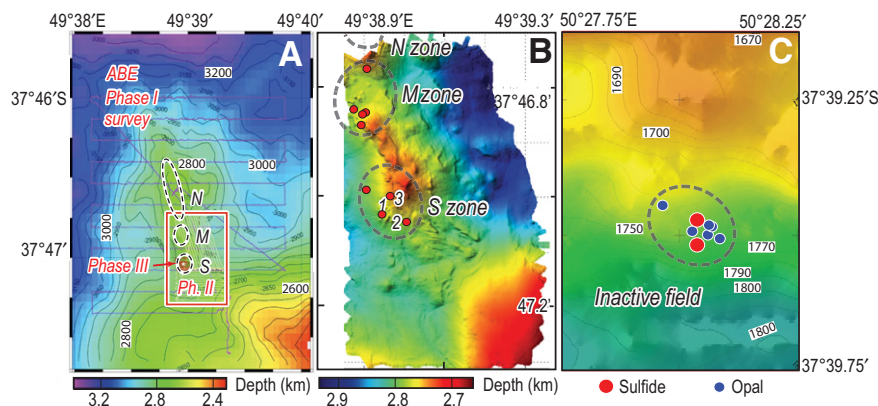


Figure 3. A: Hydrothermal activity distribution in the active and inactive vent fields. During its phase I and III dives, the autonomous underwater vehicle *ABE* (Autonomous Benthic Explorer) flew at a depth of 2625 m and 5 m from bottom, respectively, while redox potential (Eh), temperature, optical backscatter, and ADCP (acoustic Doppler current profilers) data were collected. High-resolution bathymetry and photographs were collected in phase II and III dives, respectively. **B:** Three active venting zones (S, M, and N) cover ~1000 m in distance. Red circles mark TV grab sampling positions with sulfides. Labels 1, 2, and 3 indicate the high-temperature areas. **C:** Sulfide deposits and opal distribution in the inactive field at 50°28'E.

¹GSA Data Repository item 2012013, Figures DR1–DR7, is available online at www.geosociety.org/pubs/ft2012.htm, or on request from editing@geosociety.org or Documents Secretary, GSA, P.O. Box 9140, Boulder, CO 80301, USA.

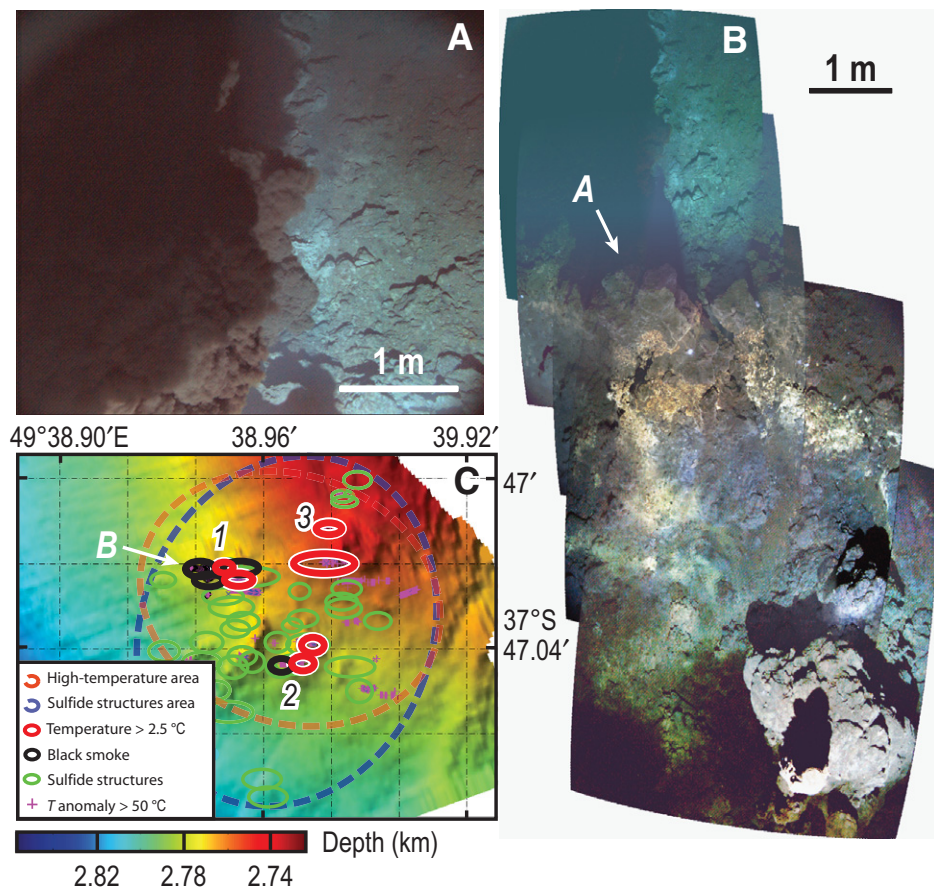


Figure 4. Details of the S zone in the active vent field. **A:** Image of a black smoker in area 1. Photo view is $\sim 4 \times 4$ m, taken from an altitude of ~ 5 m above the seafloor. **B:** Photo-mosaic showing black smoker venting (top) and sulfide deposits (lower right). **C:** Distribution of autonomous underwater vehicle *ABE* (*Autonomous Benthic Explorer*) sensor anomalies and photographed geologic features. Purple crosses indicate where temperature anomalies are >0.05 °C. Small black circles reflect optical backscatter signals >0.10 V. Dashed orange ellipse marks the estimated extent of currently active fluid flow, while dashed blue ellipse marks the estimated area of chimney structures. Green ellipses indicate the area where sulfides were obtained or observed.

its and relict chimneys are abundant throughout the S zone (green ellipses in Fig. 4C). The sampled chimneys exhibit visible zoning of distinctive mineral composition with outer portions of the conduits dominated by pyrite, marcasite, and sphalerite, while their interiors consist mainly of chalcopyrite. The texture and abundance of the chalcopyrite in this chimney material confirm a high formation temperature at this site (Tao et al., 2011). Primary analyses of selected sulfide chimney samples revealed average precious metal concentrations of Au 2.0×10^{-6} ; Ag 70.2×10^{-6} ; Cu 2.83%; Fe 31.9%; Zn 3.28%; Pb 0.01%; Co 222×10^{-6} ; and Ni 2.4×10^{-6} .

The M and N zones are located ~ 550 m and 800 m, respectively, north of the S zone (Figs. 3A–3B). Within the M zone, images of black smoke and fauna were captured using a deep-tow video sled. Fresh samples of hydrothermal chimney material were also recovered at five locations within this zone using TV grab (Fig. 3B). Their compositions are dominated by

pyrite, marcasite, sphalerite, and chalcopyrite, while two of the samples included opal. Significant in situ water-column anomalies were recorded along the western flank of the north-south-trending topographic high at $49^{\circ}39'E$, demarking the presence of a third, N, zone.

The $50^{\circ}28'E$ inactive field was detected by deep-tow video imaging and measurements of weak Eh, pH, and H_2S anomalies, as well as sampling from eight TV grab sites. It is $\sim 200 \times 125$ m in extent (Fig. 3C), similar to the S zone at $49^{\circ}39'E$. Samples collected include sulfide and opal chimneys, metalliferous sediments, basalt, and relicts of hydrothermal vent fauna. Sulfide samples were dominated by chalcopyrite, pyrite, sphalerite, and crystals of native copper. This field appears to have only become inactive recently, based on the continuing presence of abundant dead bivalve and gastropod shells. No strong turbidity anomalies were recorded in the overlying water column, arguing against the presence of any nearby, currently active black smokers.

DISCUSSIONS

Our study has revealed the first direct evidence for active venting on the SWIR, providing strong support for the hypothesis that high-temperature hydrothermal circulation is widespread along all ultraslow-spreading ridges (German et al., 1998; Baker et al., 2004), at least in the magmatically robust regions. The $49^{\circ}39'E$ active field is directly comparable, in lateral extent (at ~ 1000 m), to two of the largest known active hydrothermal fields from the slow-spreading Mid-Atlantic Ridge at TAG ($26^{\circ}N$) (Rona et al., 1986) and Rainbow ($36^{\circ}N$) (Charlou et al., 2002). Four hydrothermal sites and two hydrothermal anomalies are found in the section of the SWIR between $49^{\circ}E$ and $52^{\circ}E$. Taken together, the calculated hydrothermal site frequency along this $49^{\circ}E$ – $52^{\circ}E$ section is ~ 2.5 sites per 100 km, similar to that of the Mid-Atlantic Ridge at $36^{\circ}N$ – $38^{\circ}N$, where local magmatic supply is also robust (Baker and German, 2004). We hypothesize that local magma supply and crustal permeability play primary roles in controlling the distribution of hydrothermal activities. This implies that along slow and ultraslow ridges, the sections where excess heat is available from enhanced magmatism, but where the crust is still of suitable permeability, might be the most promising areas for searching for hydrothermal activities and sulfide deposits. Such sections could occur at distances of tens to hundreds of kilometers from hotspots.

The vent fields may provide suitable “stepping stone” niche environments that can sustain chemosynthetic ecosystems and thus enhance the potential for gene flow between the slow-spreading southern Mid-Atlantic Ridge and the medium- to fast-spreading ridge crest of the Central and Southeast Indian Ridges (Van Dover et al., 2002; Tyler et al., 2002). *ABE* photographs reveal abundant fauna in multiple locations throughout the S zone, which represent the vent-endemic taxa known from other known vent sites (Desbruyeres et al., 2006). Although dedicated biological sampling was beyond the scope of this study, organisms identified from our *ABE* seafloor photographic survey include mussels, scaly footed gastropods, stalked barnacles, and sea anemones. The scaly footed gastropod is so far known only from vents on the Central Indian Ridge (Hashimoto et al., 2001; Van Dover et al., 2001). The apparent absence of shrimp, which dominate known vents on the Mid-Atlantic Ridge (German et al., 2008) and Central Indian Ridge, is surprising and suggests that we may not have seen the full suite of biomass-dominant taxa at this site. We also did not observe the large gastropod species (*Alviniconcha* spp., *Ifremeria* spp.) that are characteristic of vents in backarc basins of the southwest Pacific Ocean (Desbruyeres et al., 2006). In that regard, this special

fauna identified in our photographic surveys at this site appears to indicate a complex affinity to vent sites on the Central Indian Ridge, the southern Mid-Atlantic Ridge (German et al., 2008), and the southwest Pacific Ocean. Clearly, sampling and analysis of these SWIR hydrothermal vent fauna will be an important priority for any future investigations of this active hydrothermal site on an ultraslow ridge.

ACKNOWLEDGMENTS

We thank the captains and crews of the DY105-17A, DY115-19, and DY115-20 cruises on R/V *Dayang Yihao*, and the *Autonomous Benthic Explorer (ABE)* group, who contributed to the success of this project. This research was funded by the China Ocean Mineral R&D Association (COMRA) project DY115-02-1, the Charles D. Hollister Endowed Fund, and the ChEss program of Woods Hole Oceanographic Institute. We are grateful to the contributions by E.T. Baker, K. Nakamura, and E. Suess for providing the Miniature Autonomous Plume Recorders, the Eh sensor, and the methane sensor, respectively. Thanks also go to Wei Huang for analysis of chimney samples and Jianping Zhou, Yonghua He, and Chunhua Gu for contributions in drafting Figures 1, 2A, 3C, DR1, and DR2.

REFERENCES CITED

- Bach, W., Banerjee, N.R., Dick, H.J.B., and Baker, E.T., 2002, Discovery of ancient and active hydrothermal systems along the ultra-slow spreading Southwest Indian Ridge 10°–16°E: *Geochemistry, Geophysics, Geosystems*, v. 3, p. 1044, doi:10.1029/2001GC000279.
- Baker, E.T., and German, C.R., 2004, On the global distribution of hydrothermal vent fields, in German, C.R., Lin, J., and Parson, L.M., eds., *Mid-Ocean Ridges: Hydrothermal Interactions between the Lithosphere and Oceans*: Washington, D.C., American Geophysical Union, p. 245–266.
- Baker, E.T., Edmonds, H.N., Michael, P.J., Bach, W., Dick, H.J.B., Snow, J.E., Walker, S.L., Banerjee, N.R., and Langmuir, C.H., 2004, Hydrothermal venting in magma deserts: The ultraslow-spreading Gakkel and Southwest Indian Ridges: *Geochemistry, Geophysics, Geosystems*, v. 5, p. Q08002, doi:10.1029/2004GC000712.
- Charlou, J.L., Donval, J.P., Fouquet, Y., Jean-Baptiste, P., and Holme, N., 2002, Geochemistry of high H₂ and CH₄ vent fluids issuing from ultramafic rocks at the Rainbow hydrothermal field (36°14'N, MAR): *Chemical Geology*, v. 191, p. 345–359, doi:10.1016/S0009-2541(02)00134-1.
- Desbruyeres, D.J., Segonzac, M., and Bright, M., 2006, *Handbook of Deep-Sea Hydrothermal Vent Fauna (2nd Completely Revised Edition)*: Denisia, Institut Français de Recherche pour l'Exploration, 544 p.
- Dick, H.J.B., Lin, J., and Schouten, H., 2003, An ultraslow-spreading class of ocean ridge: *Nature*, v. 426, p. 405–412, doi:10.1038/nature02128.
- Edmonds, H.N., Michael, P.J., Baker, E.T., Connelly, D.P., Snow, J.E., Langmuir, C.H., Dick, H.J.B., Mühe, R., German, C.R., and Graham, D.W., 2003, Discovery of abundant hydrothermal venting on the ultraslow-spreading Gakkel Ridge in the Arctic Ocean: *Nature*, v. 421, p. 252–256, doi:10.1038/nature01351.
- Fujimoto, H., Cannat, M., Fujioka, K., Gamo, T., German, C., Mével, C., Münch, U., Ohta, S., Oyaizu, M., Parson, L., Searle, R., Sohrin, Y., and Yama-shi, T., 1999, First submersible investigations of mid-ocean ridges in the Indian Ocean: *InterRidge News*, v. 8, p. 22–24.
- Georgen, J.E., Lin, J., and Dick, H.J.B., 2001, Evidence from gravity anomalies for interactions of the Marion and Bouvet hotspots with the Southwest Indian Ridge: Effects of transform offsets: *Earth and Planetary Science Letters*, v. 187, p. 283–300, doi:10.1016/S0012-821X(01)00293-X.
- German, C.R., 2003, Hydrothermal activity on the eastern Southwest Indian Ridge (50°–70°E): Evidence from core-top geochemistry, 1887 and 1998: *Geochemistry, Geophysics, Geosystems*, v. 4, p. 9103, doi:10.1029/2003GC000522.
- German, C.R., Baker, E.T., Mevel, C.A., Tamaki, K., and the FUJI Scientific Team, 1998, Hydrothermal activity along the South West Indian Ridge: *Nature*, v. 395, p. 490–493, doi:10.1038/26730.
- German, C.R., Bennett, S.A., Connelly, D.P., Evans, A.J., Murton, B.J., Parson, L.M., Prien, R.D., Ramirez-Llodra, E., Jakuba, M., Shank, T.M., Yoerger, D.R., Baker, E.T., Walker, S.L., and Nakamura, K., 2008, Hydrothermal activity on the southern Mid-Atlantic Ridge: Tectonically- and volcanically-controlled venting at 4–5°S: *Earth and Planetary Science Letters*, v. 273, p. 332–344, doi:10.1016/j.epsl.2008.06.048.
- German, C.R., and 17 others, 2010, Diverse style of submarine venting on the ultraslow spreading Mid-Cayman Rise: *Proceeding of the National Academy of Sciences of the United States of America*, p. 14020–14025, doi:10.1073/pnas.1009205107.
- Hashimoto, J., Ohta, S., Gamo, T., Chiba, H., Yamaguchi, T., Tsuchida, S., Okudaira, T., Watabe, H., Yamanaoka, T., and Kitazawa, M., 2001, First hydrothermal vent communities from the Indian Ocean discovered: *Zoological Science*, v. 18, p. 717–721, doi:10.2108/zsj.18.717.
- Herzig, P.M., and Plüger, W.L., 1988, Exploration for hydrothermal activity near the Rodriguez triple junction, Indian Ocean: *Canadian Mineralogist*, v. 26, p. 721–736.
- Lin, J., and Zhang, C., 2006, The first collaborative China-international cruises to investigate mid-ocean ridge hydrothermal vents: *InterRidge News*, v. 15, p. 33–34.
- Münch, U., Lalou, C., Halbach, P., and Fujimoto, H., 2001, Relict hydrothermal events along the super-slow Southwest Indian spreading ridge near 63°56'E—Mineralogy, chemistry and chronology of sulfide samples: *Chemical Geology*, v. 177, p. 341–349, doi:10.1016/S0009-2541(00)00418-6.
- Pedersen, R.B., Rapp, H.T., Thorseth, I.H., Lilley, M.D., Barriga, F.J.A.S., Baumberger, T., Flesland, K., Fonseca, R., Früh-Green, G.L., and Jorgensen, S.L., 2010, Discovery of a black smoker vent field and vent fauna at the Arctic mid-ocean ridge: *Nature Communications*, v. 1, Article No. 126, doi:10.1038/ncomms1124.
- Plüger, W.L., Herzig, P.M., Becker, K.P., Deissmann, G., Schops, D., Lange, L., Jenisch, A., Ladage, S., Rignow, H.H., Schulz, T., and Michaelis, W., 1990, Discovery of hydrothermal fields at the Central Indian Ridge: *Marine Mining*, v. 9, p. 73–86.
- Rona, P.A., Klinkhammer, G., Nelsen, T.A., Trefry, J.H., and Elderfield, H., 1986, Black smokers, massive sulphides and vent biota at the Mid-Atlantic Ridge: *Nature*, v. 321, p. 33–37, doi:10.1038/321033a0.
- Sauter, D., Patriat, P., Rommevaux-Jestin, C., Cannat, M., Briais, A., and Gallieni Shipboard Scientific Party, 2001, The Southwest Indian Ridge between 49°15'E and 57°E: Focused accretion and magma redistribution: *Earth and Planetary Science Letters*, v. 192, p. 303–317, doi:10.1016/S0012-821X(01)00455-1.
- Sauter, D., Carton, H., Mendel, V., Munsch, M., Rommevaux-Jestin, C., Schott, J., and Whitechurch, H., 2004, Ridge segmentation and the magnetic structure of the Southwest Indian Ridge (at 50°30'E, 55°30'E and 66°20'E): Implications for magmatic processes at ultraslow-spreading centers: *Geochemistry, Geophysics, Geosystems*, v. 5, p. Q05K08, doi:10.1029/2003GC000581.
- Scheirer, D.S., Baker, E.T., and Johnson, K.T.M., 1998, Detection of hydrothermal plumes along the Southeast Indian Ridge near the Amsterdam–St. Paul hotspot: *Geophysical Research Letters*, v. 25, p. 97–100, doi:10.1029/97GL03443.
- Snow, J.E., and Edmond, H.N., 2007, Ultraslow-spreading ridges: Rapid paradigm changes: *Oceanography (Washington, D.C.)*, v. 20, p. 90–101.
- Solomon, S., 1989, Just how do ocean ridges vary? Characteristics and population statistics of ocean ridges, in Dick, H.J.B., ed., *Drilling the Oceanic Lower Crust and Mantle: JOI/USSAC Workshop Report*: Woods Hole, Massachusetts, Woods Hole Oceanographic Institute Technical Report WHOI-89–39, p. 73–74.
- Tao, C., Wu, G., Ni, J., Zhao, H., Su, X., Zhou, N., Li, J., Chen, Y.J., Cui, R., Deng, X., Egorov, I., Dobretsova, I.G., Sun, G., Qiu, Z., Deng, X., Zhou, J., Gu, C., Li, J., Yang, J., Zhang, K., Wu, X., Chen, Z., Lei, J., Huang, W., Zhou, P., Ding, T., Jin, W., Li, H., and Lin, J., 2009, New hydrothermal fields found along the Southwest Indian Ridge during the Legs 5–7 of the Chinese DY115–20 expedition: *Eos (Transactions, American Geophysical Union)*, Fall Meeting supplement, abstract OS21A–1150.
- Tao, C., Li, H.M., Huang, W., Han, X.Q., Wu, G.H., Su, X., Zhou, N., Lin, J., He, Y.H., and Zhou, J.P., 2011, Mineralogical and geochemical features of sulfide chimney from the 49°39'E hydrothermal field on the Southwest Indian Ridge and their geological significance: *Chinese Science Bulletin*, v. 56, p. 2828–2838, doi:10.1007/s11434-011-4619-4.
- Tyler, P.A., German, C.R., Ramirez-Llodra, E., and Van Dover, C.L., 2002, *ChEss: Understanding the biogeography of chemosynthetic ecosystems: Oceanologica Acta*, v. 25, p. 227–241, doi:10.1016/S0399-1784(02)01202-1.
- Van Dover, C.L., Humphris, S.E., Fornari, D., Cavanaugh, C.M., Collier, R., Goffredi, S.K., Hashimoto, J., Lilley, M.D., Reysenbach, A.L., Shank, T.M., Von Damm, K.L., Banta, A., Gallant, R.M., Götz, D., Green, D., Hall, J., Harner, T.L., Hurtado, L.A., Johnson, P., McKiness, Z.P., Meredith, C., Olson, E., Pan, I.L., Turnipseed, M., Won, Y., Young, C.R., and Vrijenhoek, R.C., 2001, Biogeography and ecological setting of Indian Ocean hydrothermal vents: *Science*, v. 294, p. 818–823, doi:10.1126/science.1064574.
- Van Dover, C.L., German, C.R., Speer, K.G., Parson, L.M., and Vrijenhoek, R.C., 2002, Evolution and biogeography of deep-sea vent and seep invertebrates: *Science*, v. 295, p. 1253–1257, doi:10.1126/science.1067361.

Manuscript received 21 April 2011

Revised manuscript received 28 July 2011

Manuscript accepted 18 August 2011

Printed in USA

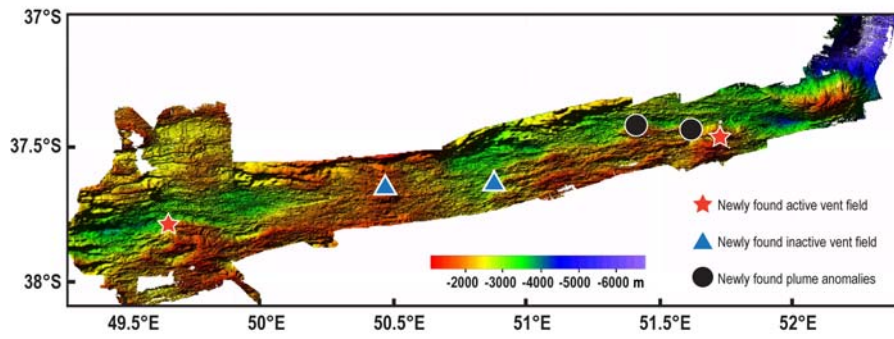


Figure DR1

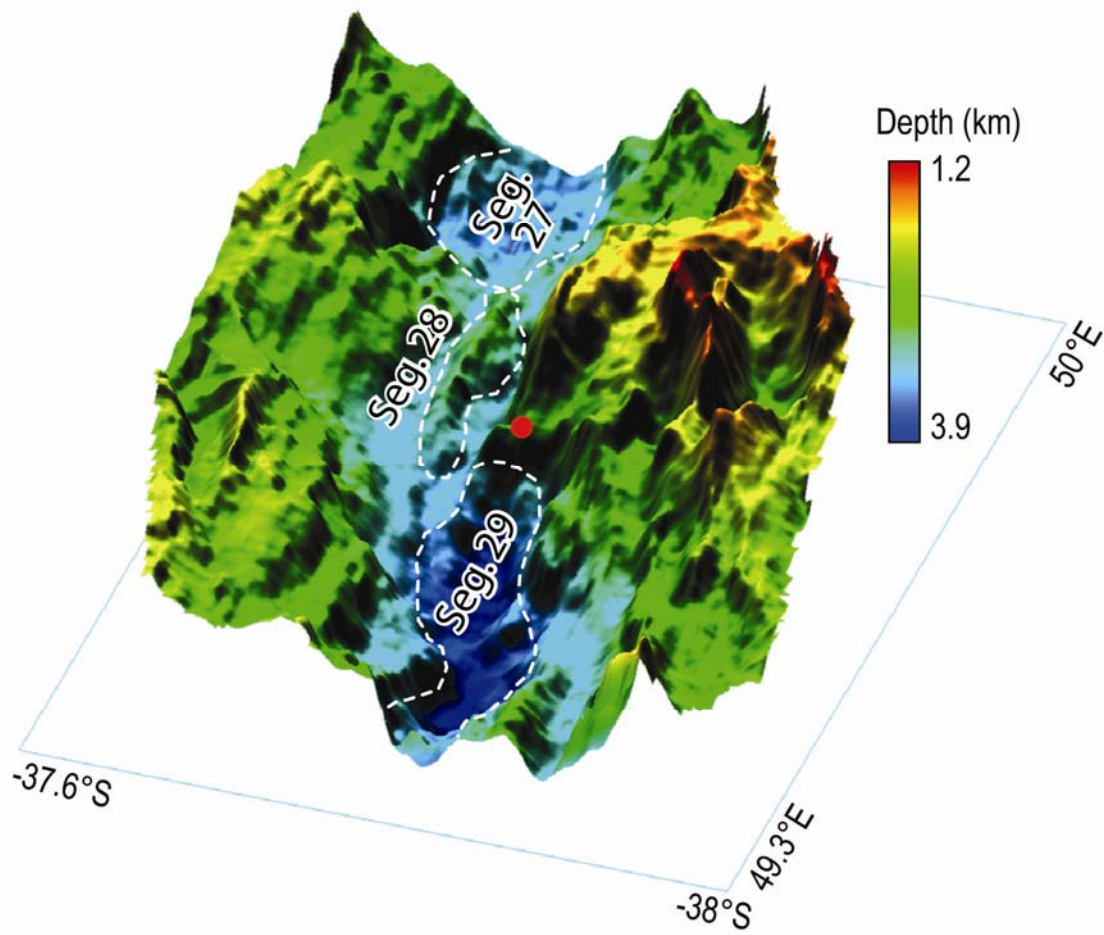


Figure DR2

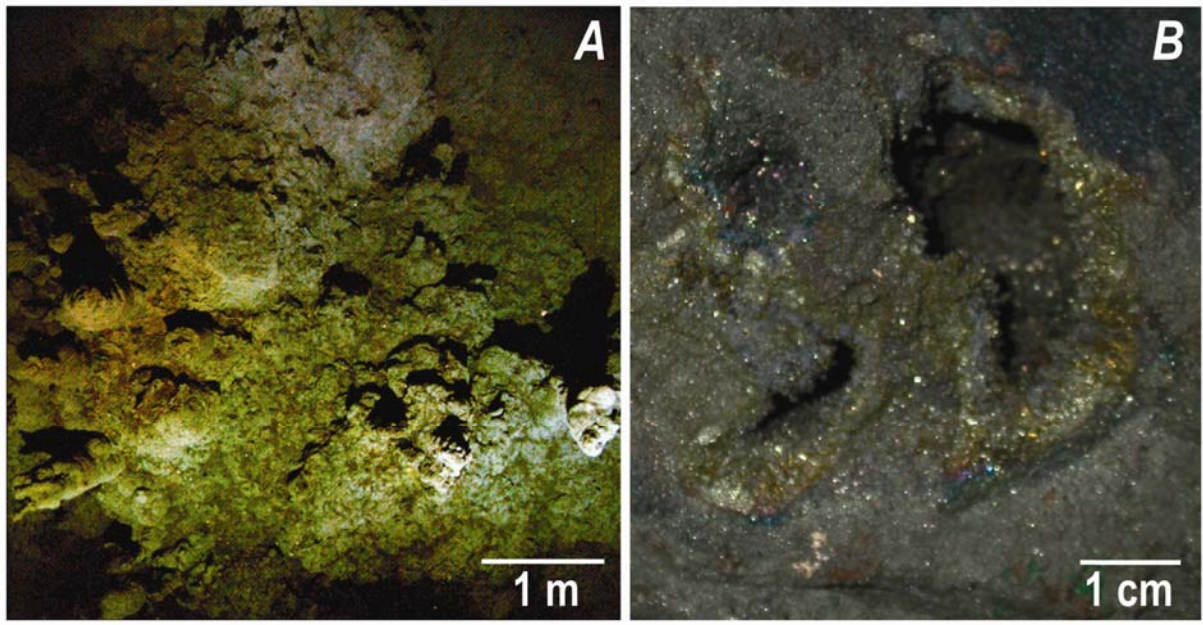


Figure DR3

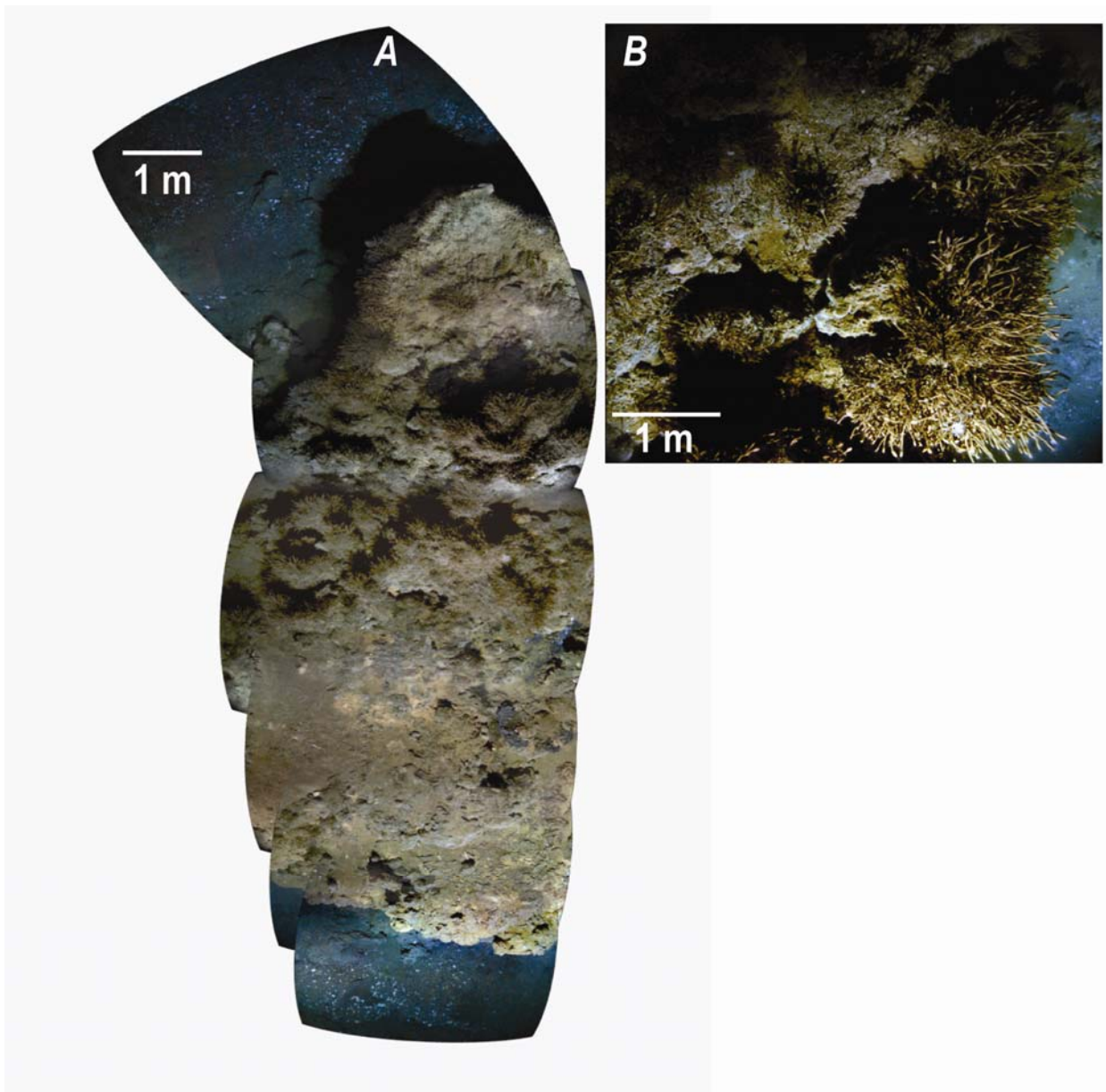


Figure DR4

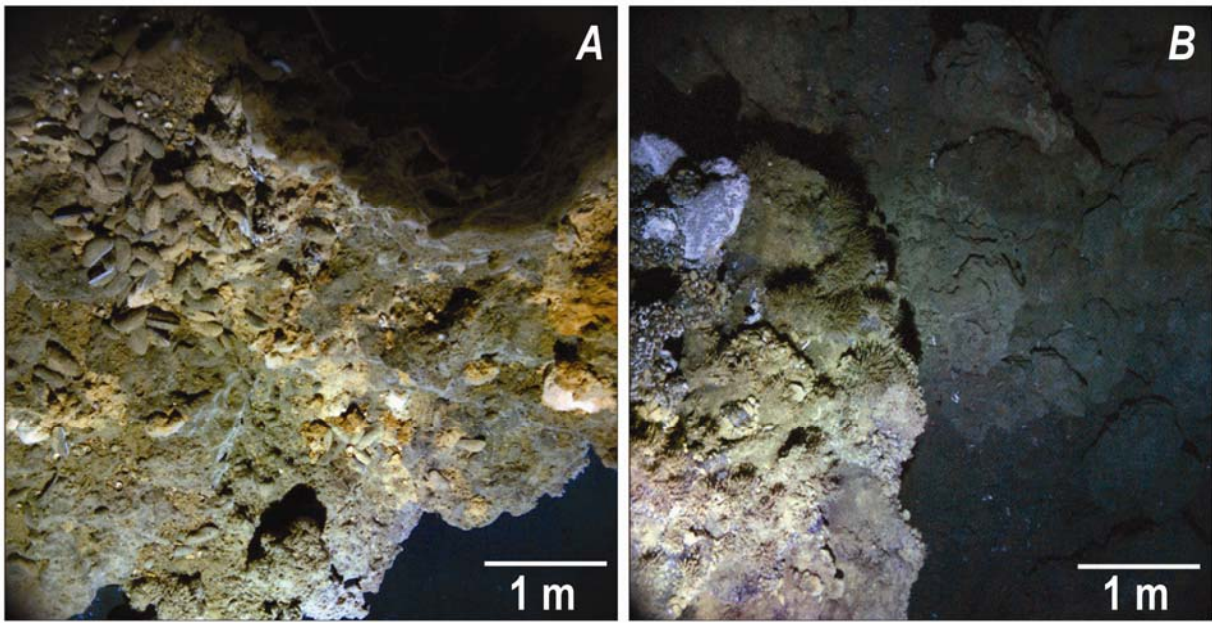


Figure DR5

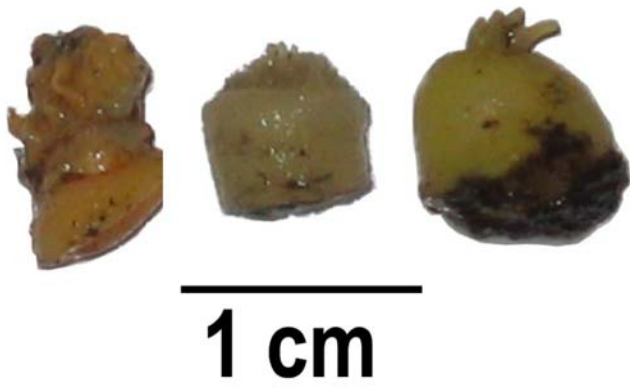


Figure DR6

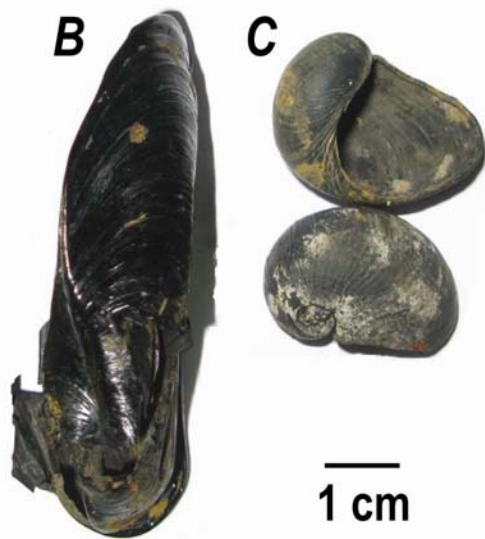
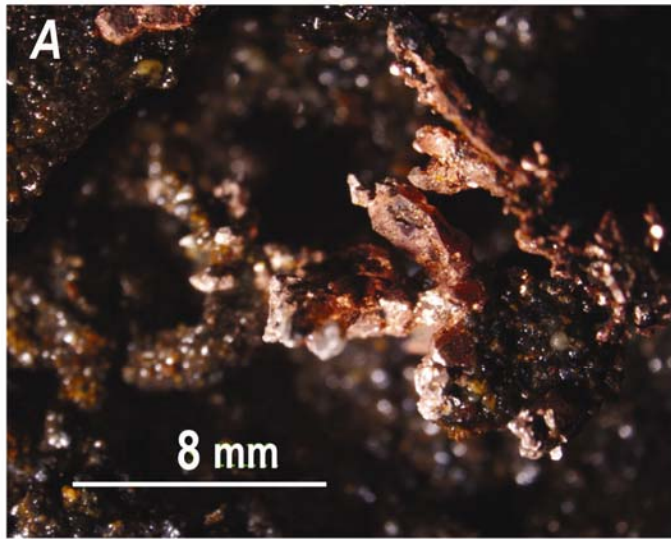


Figure DR7